Available online at www.sciencedirect.com

ScienceDirect

Procedia Manufacturing 13 (2017) 380–387

Procedia MANUFACTURING

www.elsevier.com/locate/procedia

Manufacturing Engineering Society International Conference 2017, MESIC 2017, 28-30 June 2017, Vigo (Pontevedra), Spain

An infiltration strategy to repair Carbon Fiber Reinforced Polymer (CFRP) parts

R. Garcia[a], M. Linke[b], S. Neßlinger[b], J.A. García-Manrique[a,]*

[a]*Institute of Design for Manufacturing (IDF), Universitat Politècnica de Valencia (UPV), Spain*
[b] *Hamburg University of Applied Sciences (HAW Hamburg), Hamburg, Germany,*

Abstract

This paper presents a methodology to determine the damage levels of laminate carbon fibre reinforced plastics (CFRP) parts after controlled impacts. These techniques will be used to perform a re-infiltration technique to repair composite parts and to reduce maintenance costs. It will be included the manufacturing processes, material characterization and the application of the AITM-0010 standard. Also, it is propose the use of NDT Ultrasonic inspection to determine and characterized the degree of the damage measured. This NDT method uses an advanced pulse-echo technique that through allow exploration of different angles, shapes and positions of defects.

Peer-review under responsibility of the scientific committee of the Manufacturing Engineering Society International Conference 2017.

Keywords: Fiber Reinforced Plastics, Impact Damage, Repair, Compression-After-Impact Testing, Ultrasonic Testing.

1. Introduction

Nowadays the needs to make reparations in Carbon Fiber Reinforced Polymer (CFRP) are growing, due to the high costs of manufacture and the continuous impacts that usually suffer the parts fabricated with these materials (aeronautics, wind energy, boats, automobile, etc.). The traditional method of repairing CFRPs has been to remove the damage-affected area and replace it with a patch of similar characteristics [1]. This technique needs a later finish

* Corresponding author. Tel.: +0-000-000-0000 ; fax: +0-000-000-0000 .
E-mail address: author@institute.xxx

2351-9789
Peer-review under responsibility of the scientific committee of the Manufacturing Engineering Society International Conference 2017.
10.1016/j.promfg.2017.09.024

to get surfaces free of defects. Obviously, it is a technique of high cost, but that has given satisfactory results. Its main advantage is that is certified by the aeronautical industry and therefore its use is widespread. However, this process has a number of important drawbacks, such as the time required, adds weight to the structure and the initial mechanical properties of the component cannot always be achieved.

An alternative to this CFPR parts repair process is to use a resin re-infiltration technique. This technique involves the injection of a resin of low viscosity into the damaged area by an impact. Prior to infiltration, it is necessary to know in detail the geometry of the internal damage and sometimes it is necessary to define a drilling strategy on the part to communicate all the cavities and internal cracks. In this way the re-infiltration can be made from a single injection point and one or more vents. This technique is under development and therefore is not yet certified for the civil aviation industry. Actually, this technique is allowed for performing cosmetic repairs only.

The proposal repair method based on Liquid Resin Infusion, the goal is to make the resin flow from one side of the part to the other by filling all the cracks and delaminations. The repair process includes the following steps [2]: material preparation, pre-heat of the repair components, vacuum, resin Infusion, cures

2. Materials

During this work the following materials have been used:

- Pre-impregnated biaxial fabric: Prepreg RC200T with epoxy resin (SE84 LV). It has a basis weight of 200 gr/sqm and its nominal thickness after cured is set to approximately 0.2 mm. It has a module of 72 GPa in its main direction with a fiber Vf (Fiber volume) of 58%.
- Unidirectional prepreg: Pre-impregnated fiber T700 HS with epoxy resin (SE84 LV). Its weight is 300 gr/sqm and its thickness after curing process is 0.3 mm. It has a module of 131 GPa (E1) and with a fiber Vf of 63%.

Configuration for the laminate of the test pieces: WV45/2UD0/UD90/2UD0/WV45 (WV: woven CF with 45º orientation, UD: unidirectional CF with 0º/90º orientation, Number: Indicates the number of layers when is different from one).

2.1. CFRP specimens

Using glass molds, treated with releasing agent or film, the prepreg layers were applied with previously disclosed orientations and then vacuum is applied (-1 bar). The heat-up cycle of 1° C per minute starts until the temperature reaches 80º C. With the oven stable, keeping the vacuum on for 12 hours. As shown in figure 1 the machining process of the CFRP has been carried out by means of a CNC machine of 3 axes. Six specimens (100*150 mm) taken from each “Out Of Autoclave” sheet (400 * 400 mm).

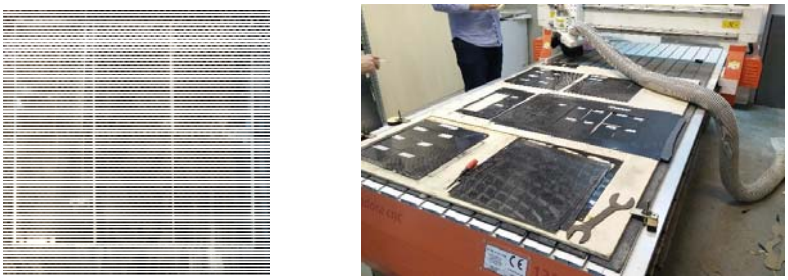

Fig. 1. Specimens

2.2. Equipment

The main equipment used has been the Drop Impact Tower, the Instron Compression After Impact Fixture and the Olympus OnmiScan SX ultrasonic scan. Figure 2 shows the OnmiScan SX the scan screen showing the data and tables 2 and 3 the parameter set-for the ultrasonic scan.

Table 1. OnmiScan SX flaw detector parameter set-up

Software	Beam delay	Start (Half Path)	Range (Half Path)	Gain	Mode
MXU 4.3R5	**17.2 µs**	**-0.41**	**4.8 mm**	**5.0 dB**	**Pulse-Eco**
Sound V.	C-Scan	A-Scan	Acquisition rate	Digitalization freq.	Reception
3000 m/s	**2.5 µs**	**10 µs**	**60**	**100 MHz**	**0º**

Table 2. Probe characterization

Model	Probe frequency	Wedge Model	Wedge Angle
5L64-NW1	**5.0 MHz**	**SNW1-0L**	**0º**

3. Methodology

This paper describes the main benefits to be obtained with these techniques, as well as their implementation. In order to certify that it is possible to repair the damage caused by impacts on structural parts, it will be used the AITM-0010 [3] standard developed by AIRBUS for this purpose and ISO 18352 [4]. The Compression After Impact test will be used. First step it will be characterize the material. The manufacturing process selected is vacuum assisted molding prepreg. In a second stage, coupons are tested in a Drop Tower for Impact Testing to develop an internal damage. Thirst internal damage is modeled with the help of Non Destructive Testing (NDT) and finally the best injection strategy will be selected to repair the material in future works. The Standard AITM 1.0010 consists of a compression test after impact. For this, composite plates (carbon fiber, glass, basalt) are used. For this test certain equipment are required to perform them.

1. Drop Impact tower (illustrated in figure 3): this machine carries out the first phase of the tests on a plate, using a projectile with determined impact energy.
2. Universal Testing Machine (Instron 5900 series): Equipment necessary to carry out the compression after impact test using the CAI fixture according with the standards [3-4].

These standards are mainly used in the aerospace industry and the impact is realized at low speed or energy. This test arises from the problem of once an impact has occurred on the piece of composite; it is possible not to see the damage with the naked eye. Therefore, it is possible that the internal damage is not detected. The most critical problem faced is the delamination, which could leads to a total loss of the properties of the composite material and its complete rupture. This test quantifies the damage produced by an impact and the energy that would remain to the material after it has been impacted.

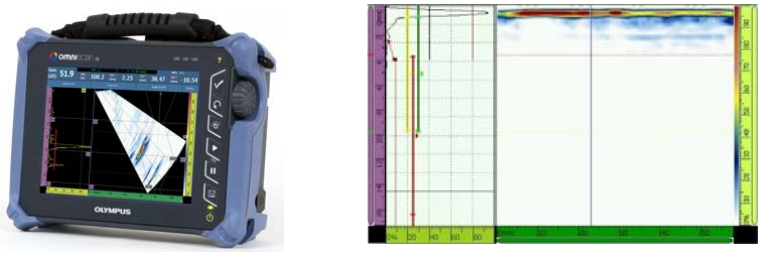

Fig. 2. Reading of pulse-echo data.

Table 3. Impact test parameters

Specimen ID	LVI03	LVI05	LVI09	LVI10	LVI12	LVI15	LVI16	LVI20	LVI25
Energy (J)	3,5	5	9	10	12	15	16	20	25
Speed (m/s)	1,34	1,61	2,16	2,27	2,49	2,78	2,87	3,21	3,59

Range of the penetration:

- Non-Visible Damage: This occurs when the impact energy is low, this damage usually translates into a delamination of the plate in its middle part. This is the most important damage since it is very difficult to detect (Figure 3, first part of the curve).
- Visible damage from the back: In this case, the damage in the piece tested begins to be visible although only on one side of the specimen. This case is also considered risk although not as much as the previous one, this is because normally in the aeronautical industry used composite panels are only visible on one side. As it can be seen in the second section of image 3 the damage produced is manifested in the opposite zone from where the impact has occurred on the specimen.
- Visible damage on both sides: This occurs when the impact energy is so high that the coupon is not able to support it. Then the damage can be considered irreparable since in the affected area there is no healthy fiber left. This part must be replaced.

3.1. Low velocity impact test

The coupons were hit with an impactor bar which is free fall accelerated through a guide. At the end of the bar, two different diameters of hemispherical nose were placed. The equipment was instrumented, registering the contact force during the impact. This process is carried out by means of a calibrated projectile of 16mm in diameter, which is dropped with a mass and height for a determined energy. At the top of the Impact Tower is the entire impact system with the projectile, additional weights and guides, at the bottom is the chamber where the coupon is positioned, and this compartment is usually under heat control to perform the tests at certain temperatures. Table 3 shows the parameters of the test such as energy, and speed.

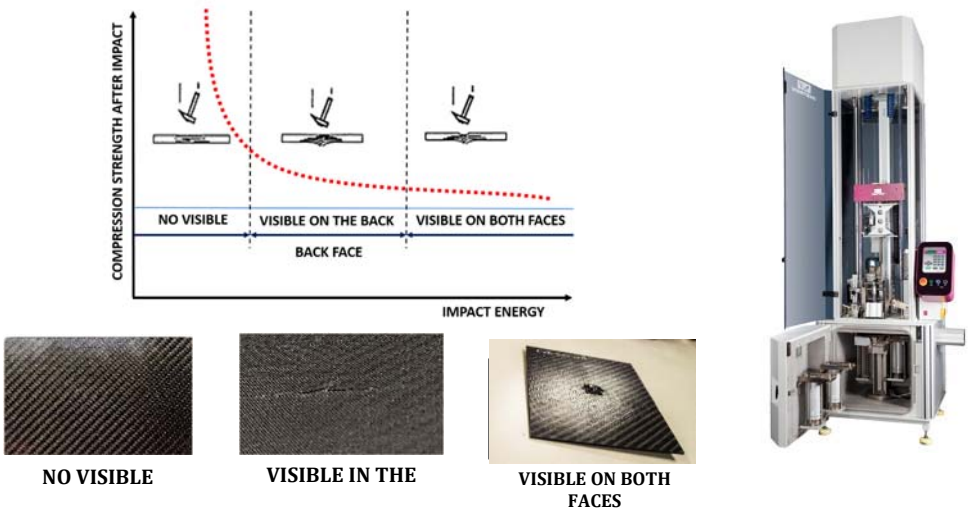

Fig. 3. Range of the penetration

3.2. Ultrasonic inspection

In order to locate the defects and the penetration ranges of the damages incurred in Drop Impact test, ultrasonic inspections was applied using an advanced pulse-echo technique. Making possible to detect fracture defects (cracks), loss of material thickness and delamination.
Thanks to the ability to transmit and receive angular and linear sound waves of zero degrees, non-destructive tests can be performed. It is used phased array probes, which is nothing more than an transducer assembly with from 8 to 64 small individual elements. Each element can be pulsed separately, sonic pulses travel through a liquid path and pass through the CFRP, and then the echoes return to the device to create an internal image that reflects the quality levels of the parts [5].

3.3. Compression After Impact (CAI)

Compression after impact tests were carried out with an Instron 5997 universal testing machine. Global bulking must be avoid and the failure is induced by the damage generated in the impact test. Then, clamping is fundamental to carry out the CAI test. The fixture function is the fastening of the coupon in the sidewalls so that there is no buckling, concentrating the damage in the middle. It is possible to control that the specimen will break through a certain area. Now it is necessary to see where the fiber will break once this compression effort is applied. Due to the definition of the laminate, the most fragile area is the one that refers to the laminate at 0°. The fibers at that angle do not oppose that applied force. Finally, it is apparent that the residual energy of these plates is between 40 and 60% of the total energy that can be absorbed by said plate. Figure 4 shows the fixture with the coupon and the damage caused by the CAI test.

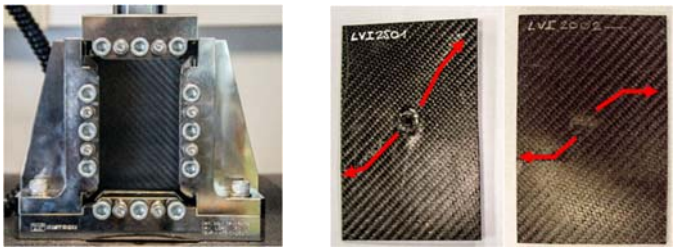

Fig. 4. Damage caused by compression – the red line indicates the break. Corresponding to the plates impact to 20 and 25 joules, which were the only ones that yielded to the compression.

It is important to remark that the compression after impact for thin carbon fiber/epoxy laminate (1,6-2,2 mm) not meets the standards [3-4], then a further work must be developed. The methodology proposed by E. Barbero could be used for this purpose. This methodology is based on the assumption that laminate failure occurs by delamination propagation perpendicular to the loading direction [6].

4. Results

The following results describes the main advantages obtained with these techniques, as well as their implementation. Representative examples of the tested specimens are presented. 5, 15 and 25 joules. Figure 6 shows the impact displacement at different impact energy. Similar behavior is observed until it is reach the 20J approximately, then the coupon collapse and the projectile crosses it (Figure 5).

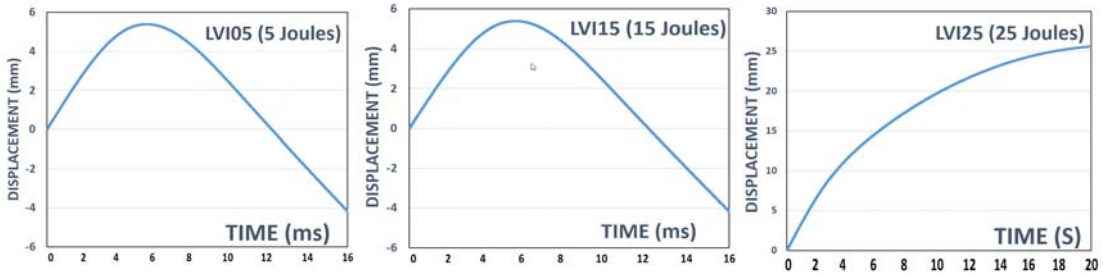

$$\vec{x} = v_0 t - \frac{1}{2}\vec{g}t^2 - \frac{1}{M}\int_0^t \int_0^t f \cdot dt$$

Fig. 5. Impact displacement for 5, 15 and 25 Joules

The impact force and velocity are represented in figure 6 and figure 7. It can be seen that the impact force is distributed between the layers. Once the layer is broken, the oscillation of the forces between layers increase and become more unstable. Once the coupon is not able to absorb the entire impact energy the absorption time is increased (Figure 7).

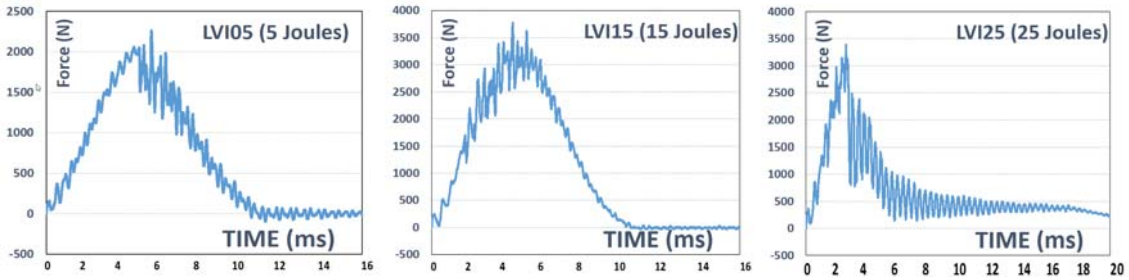

$$\vec{F} = M\vec{g} - f = \frac{\vec{dv}}{dt}$$

Fig. 6. Impact Force for 5, 15 and 25 Joules

The figure 7 shows that the impact occurs at the maximum of the velocity that is at t= 0, and then gradually reduce the velocity to 0. During this time, the energy is exchange between the impactor and the coupon. As can be seen in the last graph of figure 7, the impactor has broken the coupon and cross it since the velocity never stabilizes to zero.

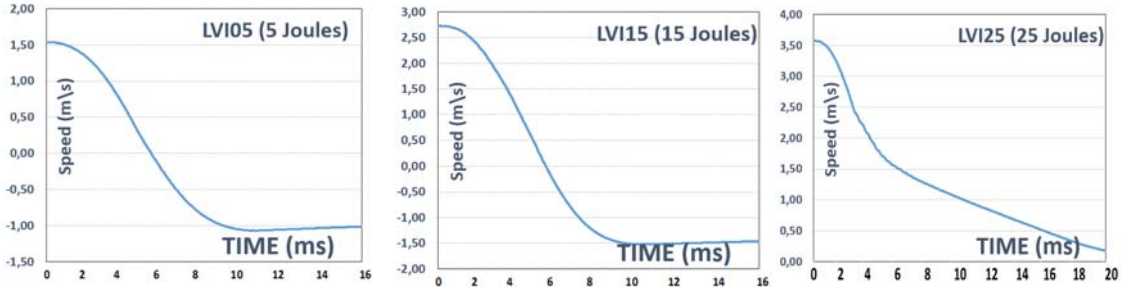

$$\vec{v} = v_0 + \vec{g}t - \frac{1}{M}\int_0^t f \cdot dt$$

Fig. 7. Impact velocity for 5, 15 and 25 Joules

The projectile break through the specimen with an energy greater than 20 joules, (figure 8). As the energy increases, the energy absorption capacity of the sheet reduce until it reaches the point of rupture.

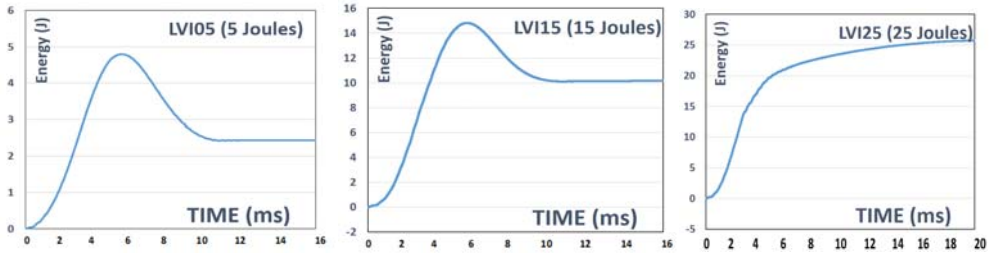

$$E = v_0 \int_0^t f \cdot dt + \vec{g} \int_0^t ft \cdot dt - \frac{1}{2M}[\int_0^t f \cdot dt]^2$$

Fig. 8. Impact bar energy for 5, 15 and 25 Joules

These results, as well as those of displacement, impact force and velocity are points of comparison for replicating the tests on repaired specimens. The specimens with external damages not visible (3 to 12 joules), are showed in figures 9-10. The figures show that they have not received internal damages that can affect their yield drastically. Thanks to depth view its perceived how increasing impact intensity start to show sign of internal damage. Knowing the magnitude of the damage is imperative in order achieving a proper repair.

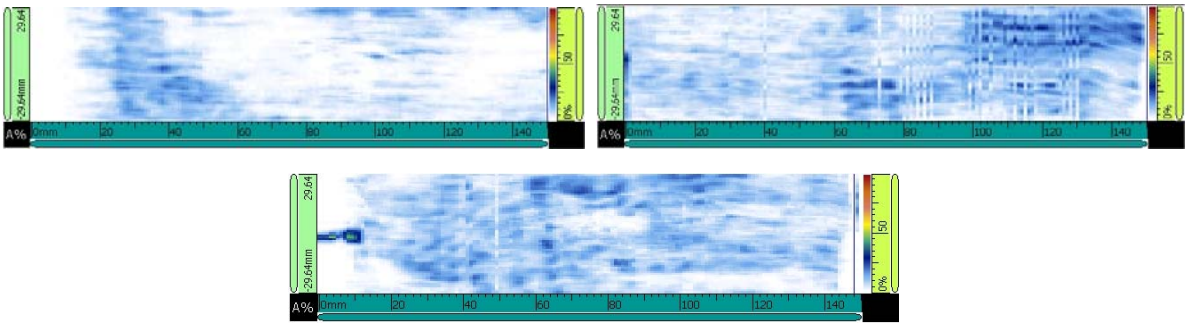

Fig. 9. LVI05, LVI10 and LVI15 specimens

Fig. 10. LVI22 specimens (Showing greater internal damage)

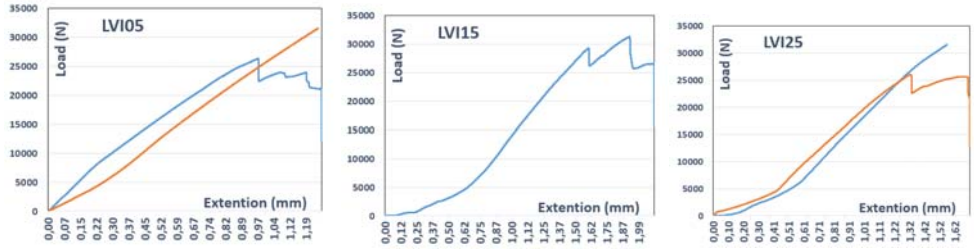

Fig. 11. Compressive load vs compressive extension graph.
(LVI05, LVI15 and LVI25 specimens)

Finally, the results of the Compression After Impact test (CAI) test are represented in figure 11 and tables 4-6

Table 4. LVI05 specimens

	Max. Compressive load (N)	Extension (mm)	Strain (MPa)	Time (s)	Vel. (mm/min)
1	26.274,54	1,34161	128,32498	116,20	0,5
2	31.494,90	1,2611	153,44653	149,31	0,5
3	31.498,72	1,28034	153,46516	153,59	0,5
AVG	29.756,06	1,29435	145,07889	139,70	0,5

Table 5. LVI15 specimens

	Max. Compressive load (N)	Extension (mm)	Strain (MPa)	Time (s)	Vel. (mm/min)
1	31.268,93	2,08487	154,41446	230,91	0,5
2	16.475,45	1,52894	81,36029	180,58	0,5
AVG	23.872,19	1,80691	117,88737	205,74	0,5

Table 6. LVI25 specimens

	Max. Compressive load (N)	Extension (mm)	Strain (MPa)	Time (s)	Vel. (mm/min)
1	31.498,98	1,58469	153,65359	188,14	0,5
2	26.020,41	1,34663	126,92885	158,96	0,5
AVG	28.759,70	1,46566	140,29122	173,55	0,5

5. Conclusions

This work aims to show the feasibility of same inspection techniques and mechanical testing to perform the re-infiltration technique for structural applications, specifically in civil aircraft. The main features will be the characterization of mechanical resistance to impact, modelling the damage using NDT and the definition of an injection strategy appropriate to each kind of crack or delamination. Further work is required to carry out the reinfiltration process with the help of the techniques shown in this paper.

Acknowledgements

The authors gratefully acknowledge the partial funding by the Federal Ministry of Education and Research of the German government under grant 03FH029AN4 and the Spanish government under DPI2013-44903-R-AR.

References

[1] K.B. Katnama, L.F.M. Da Silvab, T.M. Younga. Bonded repair of composite aircraft structures: A review of scientific challenges and opportunities. Progress in Aerospace Sciences, 61 (2013) 26–42,

[2] Lévêque, C. Huchette, P. Olivier, M. Hautier. Investigation of a Composite Repair Method by Liquid Resin Infusion. 17th International Conference on Composite Materials (2009).

[3] Airbus Industrie AITM 1.0010. Airbus Industrie Test Method. Fiber Reinforced Plastics. Determination of compression strength after Impact (1994).

[4] International Standard ISO 18352, CFRP – DETERMINATION OF COMPRESSION AFTER IMPACT PROPERTIES AT A SPECIFIED IMPACT ENERGY LEVEL (2009)

[5] T. Hasiotis, E. Badogiannis, N. Georgios. APPLICATION OF ULTRASONIC C-SCAN TECHNIQUES FOR TRACING DEFECTS IN LAMINATED COMPOSITES MATERIALS. Journal of Mechanical Engineering 57 (2001) 192-203.

[6] S. Sánchez-Sáez, E. Barbero, R. Zaera, C. Navarro. Compression after impact of thin composite laminates. Compos Sci. Tech., 65 (2005) 1911–19199.